Published in final edited form as:
J Immunol. 2016 January 1; 196(1): 256–263. doi:10.4049/jimmunol.1501140.

Priming of qualitatively superior human effector CD8+ T cells using TLR8 ligand combined with FLT3L[1]

Anna Lissina[#*,†], **Olivia Briceño**[#*,†], **Georgia Afonso**[‡,¶,§], **Martin Larsen**[*,†], **Emma Gostick**[‖], **David A Price**[‖], **Roberto Mallone**[‡,¶,§,#], and **Victor Appay**[3,*,†]

[*]Sorbonne Universités, UPMC Univ Paris 06, DHU FAST, CR7, Centre d'Immunologie et des Maladies Infectieuses (CIMI-Paris), Paris, France

[†]INSERM, U1135, CIMI-Paris, Paris, France

[‡]INSERM, U1016, Institut Cochin, Paris, France

[¶]CNRS, UMR8104, Institut Cochin, Paris, France

[§]Université Paris Descartes, Sorbonne Paris Cité, Faculté de Médecine, Paris, France

[‖]Institute of Infection and Immunity, Cardiff University School of Medicine, Cardiff, Wales, UK

[#]Assistance Publique-Hôpitaux de Paris, Hôpital Cochin, Service de Diabétologie, Paris, France

[#] These authors contributed equally to this work.

Abstract

The quality of antigen specific CD8$^+$ T cell responses is central to immune efficacy in infectious and malignant settings. Inducing effector CD8$^+$ T cells with potent functional properties is therefore a priority of immunotherapy. However, the optimal assessment of new therapeutic molecules or strategies in humans is limited by the models currently used. Here, we introduce an original model of *in vitro* CD8$^+$ T cell priming, based on an accelerated dendritic cell coculture system, which uses unfractionated human PBMCs as the starting material. This approach allows for a rapid study of adjuvant effects on the functional properties of human CD8$^+$ T cells, primed from antigen-specific naïve precursors. We demonstrate that a selective TLR8 agonist, in combination with FLT3L, primes high-quality CD8$^+$ T cell responses. TLR8L/FLT3L primed CD8$^+$ T cells displayed enhanced cytolytic activity, polyfunctionality and antigen sensitivity. The acquisition of this superior functional profile was associated with increased T-bet expression in T cells induced via an IL-12-dependent mechanism. Collectively, these data validate an expedited route to vaccine delivery or optimal T cell expansion for adoptive cell transfer.

[1]This work was supported by the French *Agence Nationale de la Recherche* (ANR; projects ANR-09-JCJC-0114-01 and ANR-14-CE14-0030-01), the *Fondation Recherche Médicale* (project DEQ20120323690), and INSERM-Transfert. DAP is a Wellcome Trust Senior Investigator and RM is an INSERM *Avenir* and APHP-INSERM *Contrat Hospitalier de Recherche Translationelle* Investigator.

[3]Address correspondence to: Victor Appay, INSERM UMRS 1135, CIMI-Paris, Hôpital Pitié-Salpêtrière, 75013 Paris, France. Facsimile: 33-1-40-77-97-34. Telephone: 33-1-40-77-81-83. victor.appay@upmc.fr.

Conflict of interest

AL, RM and VA are inventors of patent #EP14305080 entitled "Methods for testing T cell priming efficacy in a subject" filed on 21st January 2014. All other authors declare that they have no competing financial interests.

Europe PMC Funders Author Manuscripts

Keywords

CD8$^+$ T cells; Priming; TLR; Adjuvant; Immunotherapy

Introduction

Cytotoxic activity, polyfunctionality and antigen sensitivity predict CD8$^+$ T cell efficacy against infected or dysregulated cells (1, 2). Potent cytolytic activity is indeed necessary for the elimination of cancerous or infected cells. Meanwhile, demonstrations of the combined action of the cytokines interferon-γ (IFNγ) and tumour necrosis factor (TNF) in inducing permanent growth arrest in cancers, or in anti-viral processes, has highlighted the importance of T cell polyfunctionality (i.e. their capacity to produce multiple effector cytokines simultaneously) (3). Lastly, high levels of antigen sensitivity endow T cells with the capacity to recognize cognate peptide-major histocompatibility class I (pMHCI) complexes at low densities on the target cell surface, and thus to act swiftly against infected cells or to break tolerance associated with cancer (4). However, the induction of *de novo* CD8$^+$ T cell responses with such protective attributes in humans has proven difficult through vaccination (5, 6), and remains also a major goal for adoptive cell therapy. Dendritic cells (DCs) govern the nature of CD8$^+$ T cell responses primed from naïve precursors, via the provision of processed antigens in the form of pMHCI molecules, together with other important signals, including costimulatory interactions and inflammatory cytokines. Much effort has therefore been devoted to the modulation of DC function for the optimization of CD8$^+$ T cell immunity (7). Adjuvants, such as Toll-like receptor (TLR) ligands, can improve the immunogenicity of soluble protein and peptide antigens by mimicking pathogen-associated “danger” signals (8, 9), and may thus prove useful contributors to the success of immunotherapy.

However, it is difficult to study the effects of potential adjuvants on human CD8$^+$ T cell responses due to the lack of a suitable model. Although the widespread use of murine systems has greatly advanced our knowledge of TLR function and DC/T cell interactions, there are significant biological differences between mice and humans that complicate simple extrapolation between species. For instance, the cellular distribution of TLR8 is entirely different between humans and mice, and is considered to be non-functional in the latter (10). As a consequence, the adjuvant properties of TLR8-selective agonists have not been fully assessed (11, 12). Moreover, traditional *in vitro* priming protocols that use human material rely on populations of inflammatory monocyte-derived DCs (moDCs) generated in a two-stage process from peripheral blood mononuclear cell (PBMC)-purified CD14$^+$ monocytes (13). In this setting, differentiation is achieved using a combination of GM-CSF and IL-4 prior to maturation with a cocktail of inflammatory cytokines or lipopolysaccharide (LPS) (14, 15). Although adequate for many purposes, this strategy has a number of limitations. In particular, the initial preparation of moDCs is laborious and time consuming. More importantly, it is limited to one subset of antigen presenting cells, and no attempt is made to evaluate the role of conventional DCs and other resident blood cells (e.g. CD4$^+$ T cells and NK cells) in the priming process.

Europe PMC Funders Author Manuscripts

To circumvent these drawbacks, we developed an innovative model of human $CD8^+$ T cell priming. This original *in vitro* approach is based on the rapid mobilization of DCs directly from unfractionated PBMCs, adapted from an earlier method designed to detect low-frequency memory T cell responses (15). This new approach enables side-by-side studies of multiple test parameters in a standardized system with quantitative and qualitative readouts of the primed antigen-specific $CD8^+$ T cell response. Here, we used our system to compare conventional adjuvant combinations alongside the largely uncharacterized ssRNA40 TLR8 ligand (TLR8L), and to reveal the potential benefit of this agonist for the induction of high quality human effector $CD8^+$ T cells.

Materials and Methods

Flow cytometry reagents

Standard and CD8-null ELA/HLA-A2 tetramers were produced as described previously (16, 17). The CD8-null ELA/HLA-A2 complex incorporates a compound D227K/T228A mutation in the α3 domain that abrogates CD8 binding without impacting on the TCR docking platform (18). Directly conjugated monoclonal antibodies (mAbs) were purchased from commercial sources as follows: (i) α-CD8-APC-Cy7, α-CD45RA-V450, α-CCR7-PE-Cy7, α-CD107a-PE-Cy5, α-IFNγ-AlexaFluor700, α-TNF-PE-Cy7 and α-granzyme-B-V450 (BD Biosciences); (ii) α-CD3-ECD (Beckman Coulter); (iii) α-CD28-AlexaFluor700 (BioLegend); (iv) α-T-bet-AlexaFluor647 (eBiosciences); (v) α-MIP-1β-FITC (R&D Systems); (vi) α-IL-2-APC (Miltenyi Biotec); and (vii) α-perforin-BD48-FITC (Abcam). The amine-reactive viability dye Aqua (Life Technologies) was used to eliminate dead cells from the analysis. Intracellular staining for T-bet was performed using the Transcription Factor Buffer Set (BD Pharmingen) according to the manufacturer's instructions. Intracellular staining for granzyme B and perforin-BD48 was compatible with this procedure. Staining with all other reagents was conducted according to standard protocols (19, 20). Data were acquired using an LSR Fortessa flow cytometer (BD Biosciences) and analyzed with FlowJo software version 9.3.7 (TreeStar Inc.).

Peptides

All peptides were synthesized commercially at >95% purity (Biosynthesis Inc.). The ELA-10 peptide (ELAGIGILTV; Melan-A/MART-1 residues $26\text{-}35_{A27L}$) was used to pulse target cells in functional assays. The ELA-20 peptide (YTAAEELAGIGILTVILGVL; Melan-A/MART-1 residues $21\text{-}40_{A27L}$) was used for *in vitro* priming. The ELA-20Ct peptide (GHGHSYTAAEELAGIGILTV; Melan-A/MART-1 residues $16\text{-}35_{A27L}$) was tested in early presentation and stability experiments (Supplemental Figure 1).

PBMCs and cell lines

Peripheral blood mononuclear cell (PBMC) samples were obtained from healthy $HLA\text{-}A2^+$ individuals via standard protocols and cryopreserved before use in $CD8^+$ T cell priming assays. The ELA-specific $CD8^+$ T cell line Mel9916 was generated by *in vitro* priming and purified by flow cytometric sorting of ELA/HLA-A2 $tetramer^+$ events. An $HLA\text{-}A2^+$ Epstein-Barr virus (EBV)-transformed B-lymphoblastoid cell line (B-LCL) was used to present the ELA-10 peptide in activation assays. The $HLA\text{-}A2^+$ tumor cell line Me275 was

used to present the naturally processed Melan-A/MART-1 epitope (AAGIGILTV; Melan-A/MART-1 residues 27-35). The HLA-A2$^+$ Melan-A/MART-1$^-$ tumor cell line Me241 was used as a negative control.

In vitro priming of naïve Melan-A/MART-1 antigen-specific CD8$^+$ T cells

Naïve precursors specific for the HLA-A2-restricted Melan-A/MART-1 epitope ELA (ELAGIGILTV; Melan-A/MART-1 residues 26-35$_{A27L}$) were primed *in vitro* using an accelerated dendritic cell coculture protocol. Thawed PBMCs were resuspended in AIM medium (Invitrogen), supplemented with either GM-CSF (1000 IU/mL; Miltenyi Biotec) and IL-4 (500 IU/mL; Invivogen) or FLT3L (50 ng/mL; R&D Systems), and plated out at 5×10^6 cells/well in a 24-well tissue culture plate (day 0). After 24 hours (day 1), maturation of resident dendritic cells (DCs) was induced under one of the following conditions: (i) a standard cocktail of inflammatory cytokines comprising TNF (1000 U/mL), IL-1β (10 ng/mL), IL-7 (0.5 ng/mL) and prostaglandin E2 (PGE2; 1 μM) (R&D Systems) (15); (ii) LPS (0.1 μg/mL; Invivogen); or (iii) ssRNA40 (0.5 μg/mL; Invivogen). The ELA-20 peptide was added together with the DC maturation reagents at a final concentration of 1 μM. On day 2, fetal calf serum (FCS; Gibco) was added to 10% by volume per well. Fresh RPMI-1640 (Gibco) enriched with 10% FCS was used to replace the medium every 3 days. ELA-specific CD8$^+$ T cell frequency and phenotype were typically determined on day 10. Purified naïve and memory CD8$^+$ T cell subsets (Supplemental Figure 2) were obtained using the T cell Enrichment Column Kit (R&D Systems). An unconjugated α-IL-12p70 blocking antibody (R&D Systems) was added at a final concentration of 10 μg/mL on days 0, 1 and 2 in later priming experiments (Figure 6). A monoclonal mouse IgG1 isotype control antibody was used in the non-blocking conditions (α-IL-12$^-$).

Polyfunctionality assay

ELA-primed PBMCs containing approximately 5×10^4 ELA/HLA-A2 tetramer$^+$ CD8$^+$ T cells were incubated with ELA-10 peptide-pulsed HLA-A2$^+$ B-LCL target cells at an effector to target (E:T) ratio of 1:10 in the presence of α-CD107a for 6 hours at 37°C. Monensin (2.5 μg/mL; Sigma-Aldrich) and brefeldin A (5 μg/mL; Sigma-Aldrich) were added for the final 5 hours. Parallel assays were conducted with unpulsed HLA-A2$^+$ B-LCL target cells to evaluate non-specific background activation. Intracellular cytokine staining was performed as described previously (21). Data were acquired using an LSR Fortessa flow cytometer (BD Biosciences) and analyzed with FlowJo software version 9.3.7 (TreeStar Inc.). Pie charts were constructed using SPICE software (NIAID) and polyfunctionality indices were calculated as described previously (22).

Fluorometric assessment of T-lymphocyte antigen-specific lysis (FATAL) cytotoxicity assay

ELA-10 peptide-pulsed HLA-A2$^+$ B-LCL target cells were labeled with Pacific Blue succinimidyl ester (PBSE; 10 μM) to allow flow cytometric separation from unpulsed HLA-A2$^+$ B-LCL control cells, which were left unlabeled (PBSE$^-$). 10^4 PBSE$^+$ target and 10^4 PBSE$^-$ control cells were incubated with CD8-enriched PBMCs containing 5×10^4 primed ELA-specific CD8$^+$ T cells for 12 hours at 37°C. Control assays were set up in parallel either without effectors or with non-cognate CD8$^+$ T cells at the same E:T ratio (5:1). After harvesting, cells were stained with Aqua, α-CD3-ECD, α-CD8-APC-Cy7 and α-CD19-

FITC prior to acquisition using an LSR Fortessa flow cytometer (BD Biosciences). Lytic activity was calculated as a function of $PBSE^+$ target cell elimination relative to internal $PBSE^-$ control cells.

Statistical analysis

Comparisons between groups were performed using the Wilcoxon signed rank test in Prism 5 (GraphPad). P values <0.05 were considered significant.

Results

Design of an accelerated DC coculture system for the priming of T cells *in vitro*

The experimental outline of our new priming approach, starting from unfractionated PBMCs, is summarized in Figure 1A. As circulating human DCs are rare, precursors (in particular $CD14^+$ monocytes) within the starting PBMC material were mobilized using GM-CSF/IL-4 and matured with a cocktail of inflammatory cytokines including TNF, IL-1β and PGE2. IL-7 was also added to provide an additional co-stimulatory signal to naïve T cells, and facilitate their priming upon antigen-driven activation, as previously described during the optimization of our accelerated dendritic cell coculture protocol (15, 23). Alternatively, DC mobilization was achieved by exposure of PBMCs to FLT3 ligand (FLT3L), which has demonstrable T cell priming efficacy in animal studies (24). GM-CSF/IL-4 and FLT3L have been shown to act on various immune cell subsets and mobilize distinct populations of DCs (25-27). To ensure that sufficient numbers of antigen-specific $CD8^+$ T cells were present in the naïve pool for priming, we focused our analysis on the Melan-A/MART-1 epitope ($EAAGIGILTV_{26-35}$), used here as a model antigen, since it is recognized at remarkably high precursor frequencies in HLA-A*0201^+ ($HLA\text{-}A2^+$) individuals (28, 29). This large specific TCR repertoire in the naïve $CD8^+$ T cell compartment provides a useful tool for the study of human antigen-specific T cell priming. Additionally, the polyclonal nature of this Melan-A specific population presents an advantage over the TCR transgenic experimental mouse models that are typically employed for the study antigen-driven adaptive immunity (30, 31). To ensure optimal immunogenicity, we used the heteroclitic sequence of the epitope: ELAGIGILTV (ELA) (32). Moreover, the ELA epitope was incorporated into a 20mer synthetic long peptide (SLP, ELA-20) as a means of limiting antigen display to DCs with cross-presentation capacity (33-35). Prior to experimentation, we verified that the ELA-20 peptide required active processing. Specifically, we showed that ELA-20 was not presented directly by HLA-A2 (Supplemental Figure 1A) and was not subjected to non-specific cleavage by enzymes present in serum (Supplemental Figure 1B).

Next, we evaluated the optimal parameters for ELA-specific $CD8^+$ T cell priming in our system. An ELA-20 concentration of 1 μM consistently generated sufficiently large populations of primed cells for functional characterization (data not shown), and was therefore chosen for all downstream assays. Primed ELA-specific $CD8^+$ T cells peaked on day 10 (Figure 1B), following identical kinetics and achieving comparable magnitudes with both the GM-CSF/IL-4 and FLT3L protocols (Supplemental Figure 2A). Subsequent experiments were therefore conducted over this time frame. We also confirmed that primed ELA-specific $CD8^+$ T cells originated from the naïve pool, by showing that ELA/HLA-A2

tetramer$^+$ T cells were expanded from purified naïve (CCR7$^+$ CD45RA$^+$) but not memory CD8$^+$ T cells (Supplemental Figures 2B and 2C). After priming, the vast majority of ELA/HLA-A2 tetramer$^+$ CD8$^+$ T cells displayed phenotypic hallmarks of antigen-driven expansion, predominantly differentiating into the effector memory (CCR7$^-$ CD45RA$^-$) compartment (Supplemental Figures 2D and 2E). No differences in terms of differentiation status were observed between ELA-specific CD8$^+$ T cell populations primed with either GM-CSF/IL-4 or FLT3L (Supplemental Figure 2E).

Human CD8$^+$ T cell priming with a TLR8 selective agonist

In subsequent experiments, we used our validated system to study the effect of a recently available TLR8L (ssRNA40), in comparison with the standard cocktail of inflammatory cytokines (TNF, IL-1β, PGE2 and IL-7), or with LPS, an extensively studied TLR4 ligand (TLR4L). Either TLR4L or TLR8L was introduced during the DC maturation step, *in lieu* of the inflammatory cytokine cocktail. Tetramer-based enumeration of ELA-specific CD8$^+$ T cell populations expanded in parallel revealed no major differences in the magnitude of priming across the three maturation conditions tested (Figure 1C). However, the GM-CSF/IL-4/TLR8L combination primed significantly fewer ELA-specific CD8$^+$ T cells compared to the FLT3L/TLR8L combination, highlighting differences in the way that GM-CSF/IL-4 and FLT3L modulate subsets of antigen-presenting cells. To support this point, we subjected purified CD14$^+$ monocytes to GM-CSF/IL-4 or FLT3L, before introducing different maturation factors into the culture medium (Supplemental Figure 3). As expected, GM-CSF/IL-4 but not FLT3L, treatment resulted in the differentiation of the monocytes into moDCs (with the downregulation of CD14 from the surface of GM-CSF/IL-4 treated cells). However, while our cytokine cocktail or TLR4L induced the maturation of these cells (measured by the upregulation of HLA-DR and CD86 on the surface of moDCs), TLR8L had no effect. The failure of GM-CSF/IL-4-induced moDCs to respond to TLR8L stimulation (despite them being known to express TLR8), provides one potential explanation for the poor T cell priming capacity of the GM-CSF/IL-4/TLR8L combination in our system. These findings highlight the limitations of the widespread use of moDCs, and question the suitability of these *in vitro* generated inflammatory cells for the study of potential adjuvants. This observation provides an additional argument in favour of using a system of unfractionated PBMCs as an alternative to isolated moDCs, the use of which would have overlooked the FLT3L/TLR8L effect on T cell priming. Notably, the FLT3L/TLR8L-primed ELA-specific CD8$^+$ T cells possessed significantly greater cytotoxic potential, assessed by the expression of granzyme B and perforin, than cells primed in the other conditions (Figures 2A and 2B). This observation was confirmed in antigen-presenting cell lysis assays, whereby CD8$^+$ T cells primed in the presence of FLT3L/TLR8L, killed more than twice as many target cells loaded with 1 μM ELA-10 than was achieved by CD8$^+$ T cells primed under any other condition (Figures 2C and 2D). Moreover, only FLT3L/TLR8L-primed CD8$^+$ T cells were capable of eliminating targets presenting ELA-10 at a concentration of 10 nM.

Qualitatively superior human CD8+ T cell responses primed with an FLT3L/TLR8L combination

Next, we assessed the ability of primed $CD8^+$ T cells to deploy multiple effector functions in response to antigen encounter. In these assays, we measured the simultaneous induction of IFNγ, MIP-1β, TNF and IL-2, together with surface mobilization of CD107a (Figure 3A). Although GM-CSF/IL-4 and FLT3L in conjunction with the cytokine cocktail generated ELA-primed $CD8^+$ T cells expressing similar levels of cytotoxic molecules (Figures 2A and 2B), FLT3L treatment elicited greater frequencies of polyfunctional cells compared to GM-CSF/IL-4 (Figure 3B top row). Moreover, ELA-specific $CD8^+$ T cells primed using the FLT3L/TLR8L combination displayed the highest levels of polyfunctionality (Figure 3B). These differences were statistically significant in terms of the calculated polyfunctionality index across individual PBMC donors (Figure 3C).

Antigen sensitivity, a major determinant of $CD8^+$ T cell functional attributes, was evaluated via cognate peptide titration in IFNγ secretion assays. FLT3L/TLR8L-primed ELA-specific $CD8^+$ T cells displayed the highest antigen sensitivity, with a typical EC50 value (7.45×10^{-9} M) approximately one or two orders of magnitude lower compared to the GM-CSF/IL-4/TLR4L (5.77×10^{-8} M) or FLT3L/cytokine (1.36×10^{-7} M) combinations, respectively (Figure 4A). IFNγ production by GM-CSF/IL-4/cytokine-primed ELA-specific $CD8^+$ T cells was negligible. These differences in antigen sensitivity between conditions extended across the full spectrum of effector functions, enabling FLT3L/TLR8L-primed $CD8^+$ T cells to deploy multiple effector functions at ELA-10 peptide concentrations as low as 1 nM (Figure 4B), equivalent to the amount of antigen presented in physiological settings. Crucially, FLT3L/TLR8L-primed ELA-specific $CD8^+$ T cells were indeed capable of mounting polyfunctional responses to an $HLA\text{-}A2^+$ melanoma cell line naturally expressing the endogenous Melan-A/MART-1 antigen (Figure 4C). In contrast, the same tumor cell line was not recognized efficiently by ELA-specific $CD8^+$ T cells primed under other test conditions (Figure 4C).

Mechanistic insights into TLR8L mediated adjuvant effects

We then decided to explore the mechanisms involved in the acquisition of superior functional attributes by FLT3/TLR8L-primed $CD8^+$ T cells. It is established that T cell receptor (TCR) avidity, defined as the collective affinities of multiple monomeric TCR/pMHC interactions, can greatly influence antigen sensitivity and thereby dictate the functional profile of $CD8^+$ T cells in response to cognate antigen (21, 36). Accordingly, we used standard and CD8-null ELA/HLA-A2 tetramers in parallel to quantify this parameter across different priming conditions (Figure 5A). CD8-null tetramers are characterized by their inability to bind the CD8 coreceptor, thereby enabling the selective detection of high avidity cells among total antigen-specific $CD8^+$ T cells (identified with standard reagents) (17). Besides a small increase in TCR avidity within the FLT3/TLR8L-primed $CD8^+$ T cell population, no statistically significant differences in TCR avidity were detected across any of the test conditions (Figure 5B).

The expression of effector molecules such as granzyme B, perforin and IFNγ is tightly controlled in $CD8^+$ T cells by the T-box transcription factor T-bet (also known as Tbx-21)

(37). We therefore assessed the intracellular expression of T-bet in $CD8^+$ T cells upon priming. Significantly higher T-bet expression levels were detected in ELA-specific $CD8^+$ T cells primed with FLT3L/TLR8L compared to other combinations (Figures 5C and 5D). An important regulator of T-bet expression is IL-12 (38), which is known to be secreted by myeloid DCs upon TLR8 ligation (11). To assess the relationship between IL-12 levels and T-bet induction in our *in vitro* priming system, an α-IL-12p70 blocking antibody was administered daily during the first three days of culture. This intervention led to a significant drop in T-bet levels in FLT3L/TLR8L-primed $CD8^+$ T cells (Figures 6A and 6B). Moreover, ELA-specific $CD8^+$ T cells primed in the presence of the α-IL-12p70 blocking antibody expressed considerably less granzyme B and perforin (Figure 6C), and were also less polyfunctional (Figure 6D). In our system, IL-12 appears therefore to be a key factor for driving T-bet expression in $CD8^+$ T cells primed in the presence of TLR8L, and consequently an indirect enhancer of their effector functions.

Discussion

We report here that human PBMCs mobilized with GM-CSF/IL-4 or FLT3L responded differently to maturation signals such as cytokines or TLR ligands, affecting the quality of the primed $CD8^+$ T cell responses. Importantly, the combined use of FLT3L and TLR8L resulted in the priming of antigen-specific $CD8^+$ T cells displaying robust effector functions, showing for the first time that a selective TLR8 agonist can act as a potent adjuvant to prime functionally superior antigen-specific human $CD8^+$ T cells. Collectively, our data indicate that TLR8L, through effects on FLT3L (but not GM-CSF/IL-4) -mobilized DCs, triggers T-bet expression in primed $CD8^+$ T cells through an IL-12 dependent mechanism. In turn, T-bet endows these $CD8^+$ T cells with superior antigen sensitivity, robust cytolytic activity and polyfunctionality. We also demonstrate that the high antigen sensitivity of FLT3L/TLR8L-primed $CD8^+$ T cells does not arise through the selection of T cells bearing high avidity TCRs during the priming process. Instead, this gain in antigen sensitivity may be explained by a reduction in TCR/pMHCI activation thresholds experienced by FLT3L/TLR8L primed cells (due to heightened T-bet expression, induced by IL-12), leaving them poised for antigen-driven activation.

These new findings were made possible owing to the development of an original *in vitro* priming model that offers several practical and theoretical advantages over existing systems. In addition to streamlining the search for more effective adjuvants, our approach is applicable to several notable challenges in the field. The use of unmanipulated PBMCs (which also includes cord or elderly blood samples) in our system will likely aid in the identification of immunization regimens suitable for individuals who are typically refractory to priming with standard vaccines, for instance at the extremes of age or with advanced HIV infection. Moreover, our priming model can be of use to the study of mechanisms underlying effective T cell priming (e.g. to identify the DC subsets or molecular pathways involved). For instance, preliminary data using our approach imply that DCs from the myeloid lineage are most likely to be involved in FLT3L/TLR8L-mediated T cell priming. In contrast to the GMCSF receptor (CD116), FLT3 (CD135) was not expressed on $CD14^+$ monocytes, but was instead localised to plasmacytoid and myeloid DCs (pDCs and mDCs, respectively, data not shown), implicating these DC subsets in the FLT3L-mediated priming

process. Furthemore, experiments involving the magnetic depletion of various microbead-bound antigen presenting cell subsets prior to priming initiation showed no influence of $CD14^+$ monocytes or pDCs on ELA-specific $CD8^+$ T cell priming with the FLT3L/TLR8L combination. Meanwhile, the depletion of mDCs had a negative impact on priming (carried out in the presence of FLT3L and TLR8L) in some experiments, suggesting a potential involvement of mDCs (data now shown). Overall, we view it as being likely that mDCs (rather than pDCs) play at least a partial role in $CD8^+$ T cell priming in the presence of FLT3L and TLR8L, consistent with the fact that TLR8 is expressed by mDCs, but not pDCs. However, it is highly likely that other DC subsets hold the potential to prime $CD8^+$ T cells in these same culture conditions. For instance, FLT3L was recently reported to mobilize a rare population of circulating mDC precursors (39), which could play this role. Finally, our model could also facilitate the selection of antigen formulations best suited to the induction of highly functional *de novo* T cell responses. The use of SLPs, which display several beneficial features for $CD8^+$ T cell priming compared to short peptides (34, 35, 40, 41), serves as one such example.

We envisage that the *in vitro* priming approach presented in this study is useful for screening candidate antigens and adjuvants for vaccination in humans. For instance, the present data encourage further testing of the adjuvant potential and inflammatory properties of a selective TLR8 agonist in *in vivo* models. Recent work in transgenic mice, expressing different levels of human TLR8, supports a role for this receptor in autoimmune inflammation, advocating potentially adverse effects of TLR8L use in humans (42). However, these inflammatory side-effects may be averted through the specific targeting of such an adjuvant directly to lymph nodes, using delivery agents such as amphiphiles (i.e. linking the antigen and adjuvant to a lipophilic albumin-binding tail) or nanoparticles (43, 44). These approaches could be called upon to decrease the systemic dissemination and potential toxicity of TLR8L, while boosting $CD8^+$ T cell priming efficacy. In light of our findings, investigating the adjuvant potential of other TLR8 (e.g. ssPoly(U) or benzoazepine analog TL8-506) or TLR7/8 (e.g. imidazoquinoline R848 or thiazoquinolone CL075) specific ligands using our approach will be important. Differences in potency or unexpected antagonizing effects (e.g. between TLR7 and TLR8 signalling pathways) might be observed. The present *in vitro* priming system may also expedite the generation of potent T cells for adoptive cell therapy. It is notable in this respect that FLT3L/TLR8L-primed antigen-specific $CD8^+$ T cells recognized naturally presented antigens on a tumor cell line and exhibited properties associated with *in vivo* efficacy. Overall, the present findings are directly relevant to our understanding of effector T cell generation and the development of effective immunotherapy in humans.

Supplementary Material

Refer to Web version on PubMed Central for supplementary material.

Acknowledgements

We thank Pedro Romero for providing melanoma cell lines and Robert Seder for constructive discussions.

References

1. Appay V, Douek DC, Price DA. CD8+ T cell efficacy in vaccination and disease. Nat Med. 2008; 14:623–628. [PubMed: 18535580]
2. Seder RA, Darrah PA, Roederer M. T-cell quality in memory and protection: implications for vaccine design. Nat Rev Immunol. 2008; 8:247–258. [PubMed: 18323851]
3. Braumuller H, Wieder T, Brenner E, Assmann S, Hahn M, Alkhaled M, Schilbach K, Essmann F, Kneilling M, Griessinger C, Ranta F, Ullrich S, Mocikat R, Braungart K, Mehra T, Fehrenbacher B, Berdel J, Niessner H, Meier F, van den Broek M, Haring HU, Handgretinger R, Quintanilla-Martinez L, Fend F, Pesic M, Bauer J, Zender L, Schaller M, Schulze-Osthoff K, Rocken M. T-helper-1-cell cytokines drive cancer into senescence. Nature. 2013; 494:361–365. [PubMed: 23376950]
4. Dutoit V, Rubio-Godoy V, Dietrich PY, Quiqueres AL, Schnuriger V, Rimoldi D, Lienard D, Speiser D, Guillaume P, Batard P, Cerottini JC, Romero P, Valmori D. Heterogeneous T-cell response to MAGE-A10(254-262): high avidity-specific cytolytic T lymphocytes show superior antitumor activity. Cancer Res. 2001; 61:5850–5856. [PubMed: 11479225]
5. Rosenberg SA, Yang JC, Restifo NP. Cancer immunotherapy: moving beyond current vaccines. Nat Med. 2004; 10:909–915. [PubMed: 15340416]
6. Pulendran B, Ahmed R. Immunological mechanisms of vaccination. Nat Immunol. 2011; 12:509–517. [PubMed: 21739679]
7. Banchereau J, Palucka AK. Dendritic cells as therapeutic vaccines against cancer. Nat Rev Immunol. 2005; 5:296–306. [PubMed: 15803149]
8. Kawai T, Akira S. The role of pattern-recognition receptors in innate immunity: update on Toll-like receptors. Nat Immunol. 2010; 11:373–384. [PubMed: 20404851]
9. Coffman RL, Sher A, Seder RA. Vaccine adjuvants: putting innate immunity to work. Immunity. 2010; 33:492–503. [PubMed: 21029960]
10. Jurk M, Heil F, Vollmer J, Schetter C, Krieg AM, Wagner H, Lipford G, Bauer S. Human TLR7 or TLR8 independently confer responsiveness to the antiviral compound R-848. Nat Immunol. 2002; 3:499. [PubMed: 12032557]
11. Gorden KB, Gorski KS, Gibson SJ, Kedl RM, Kieper WC, Qiu X, Tomai MA, Alkan SS, Vasilakos JP. Synthetic TLR agonists reveal functional differences between human TLR7 and TLR8. J Immunol. 2005; 174:1259–1268. [PubMed: 15661881]
12. Steinhagen F, Kinjo T, Bode C, Klinman DM. TLR-based immune adjuvants. Vaccine. 2011; 29:3341–3355. [PubMed: 20713100]
13. Sallusto F, Lanzavecchia A. Efficient presentation of soluble antigen by cultured human dendritic cells is maintained by granulocyte/macrophage colony-stimulating factor plus interleukin 4 and downregulated by tumor necrosis factor alpha. J Exp Med. 1994; 179:1109–1118. [PubMed: 8145033]
14. Wolfl M, Greenberg PD. Antigen-specific activation and cytokine-facilitated expansion of naive, human CD8+ T cells. Nature protocols. 2014; 9:950–966. [PubMed: 24675735]
15. Martinuzzi E, Afonso G, Gagnerault MC, Naselli G, Mittag D, Combadiere B, Boitard C, Chaput N, Zitvogel L, Harrison LC, Mallone R. acDCs enhance human antigen-specific T-cell responses. Blood. 2011; 118:2128–2137. [PubMed: 21715316]
16. Altman JD, Moss PAH, Goulder PJR, Barouch DH, McHeyzer-Williams MG, Bell JI, McMichael AJ, Davis MM. Phenotypic analysis of antigen-specific T lymphocytes [published erratum appears in Science 1998 Jun 19;280(5371):1821]. Science. 1996; 274:94–96. [PubMed: 8810254]
17. Price DA, Brenchley JM, Ruff LE, Betts MR, Hill BJ, Roederer M, Koup RA, Migueles SA, Gostick E, Wooldridge L, Sewell AK, Connors M, Douek DC. Avidity for antigen shapes clonal dominance in CD8+ T cell populations specific for persistent DNA viruses. J Exp Med. 2005; 202:1349–1361. [PubMed: 16287711]
18. Purbhoo MA, Boulter JM, Price DA, Vuidepot AL, Hourigan CS, Dunbar PR, Olson K, Dawson SJ, Phillips RE, Jakobsen BK, Bell JI, Sewell AK. The human CD8 coreceptor effects cytotoxic T cell activation and antigen sensitivity primarily by mediating complete phosphorylation of the T cell receptor zeta chain. J Biol Chem. 2001; 276:32786–32792. [PubMed: 11438524]

19. Whelan JA, Dunbar PR, Price DA, Purbhoo MA, Lechner F, Ogg GS, Griffiths G, Phillips RE, Cerundolo V, Sewell AK. Specificity of CTL interactions with peptide-MHC class I tetrameric complexes is temperature dependent. J Immunol. 1999; 163:4342–4348. [PubMed: 10510374]

20. Papagno L, Almeida JR, Nemes E, Autran B, Appay V. Cell permeabilization for the assessment of T lymphocyte polyfunctional capacity. J Immunol Methods. 2007; 328:182–188. [PubMed: 17920073]

21. Almeida JR, Sauce D, Price DA, Papagno L, Shin SY, Moris A, Larsen M, Pancino G, Douek DC, Autran B, Saez-Cirion A, Appay V. Antigen sensitivity is a major determinant of CD8+ T-cell polyfunctionality and HIV-suppressive activity. Blood. 2009; 113:6351–6360. [PubMed: 19389882]

22. Larsen M, Sauce D, Arnaud L, Fastenackels S, Appay V, Gorochov G. Evaluating cellular polyfunctionality with a novel polyfunctionality index. PLoS One. 2012; 7:e42403. [PubMed: 22860124]

23. Martinuzzi E, Scotto M, Enee E, Brezar V, Ribeil JA, van Endert P, Mallone R. Serum-free culture medium and IL-7 costimulation increase the sensitivity of ELISpot detection. J Immunol Methods. 2008; 333:61–70. [PubMed: 18242633]

24. Guermonprez P, Helft J, Claser C, Deroubaix S, Karanje H, Gazumyan A, Darasse-Jeze G, Telerman SB, Breton G, Schreiber HA, Frias-Staheli N, Billerbeck E, Dorner M, Rice CM, Ploss A, Klein F, Swiecki M, Colonna M, Kamphorst AO, Meredith M, Niec R, Takacs C, Mikhail F, Hari A, Bosque D, Eisenreich T, Merad M, Shi Y, Ginhoux F, Renia L, Urban BC, Nussenzweig MC. Inflammatory Flt3l is essential to mobilize dendritic cells and for T cell responses during Plasmodium infection. Nat Med. 2013; 19:730–738. [PubMed: 23685841]

25. Pulendran B, Banchereau J, Burkeholder S, Kraus E, Guinet E, Chalouni C, Caron D, Maliszewski C, Davoust J, Fay J, Palucka K. Flt3-ligand and granulocyte colony-stimulating factor mobilize distinct human dendritic cell subsets in vivo. J Immunol. 2000; 165:566–572. [PubMed: 10861097]

26. Parajuli P, Mosley RL, Pisarev V, Chavez J, Ulrich A, Varney M, Singh RK, Talmadge JE. Flt3 ligand and granulocyte-macrophage colony-stimulating factor preferentially expand and stimulate different dendritic and T-cell subsets. Exp Hematol. 2001; 29:1185–1193. [PubMed: 11602320]

27. Xu Y, Zhan Y, Lew AM, Naik SH, Kershaw MH. Differential development of murine dendritic cells by GM-CSF versus Flt3 ligand has implications for inflammation and trafficking. J Immunol. 2007; 179:7577–7584. [PubMed: 18025203]

28. Pittet MJ, Valmori D, Dunbar PR, Speiser DE, Lienard D, Lejeune F, Fleischhauer K, Cerundolo V, Cerottini JC, Romero P. High frequencies of naive Melan-A/MART-1-specific CD8(+) T cells in a large proportion of human histocompatibility leukocyte antigen (HLA)-A2 individuals. J Exp Med. 1999; 190:705–715. [PubMed: 10477554]

29. Dutoit V, Rubio-Godoy V, Pittet MJ, Zippelius A, Dietrich PY, Legal FA, Guillaume P, Romero P, Cerottini JC, Houghten RA, Pinilla C, Valmori D. Degeneracy of antigen recognition as the molecular basis for the high frequency of naive A2/Melan-a peptide multimer(+) CD8(+) T cells in humans. J Exp Med. 2002; 196:207–216. [PubMed: 12119345]

30. Pinto S, Sommermeyer D, Michel C, Wilde S, Schendel D, Uckert W, Blankenstein T, Kyewski B. Misinitiation of intrathymic MART-1 transcription and biased TCR usage explain the high frequency of MART-1-specific T cells. Eur J Immunol. 2014; 44:2811–2821. [PubMed: 24846220]

31. Romero P, Speiser DE, Rufer N. Deciphering the unusual HLA-A2/Melan-A/MART-1-specific TCR repertoire in humans. Eur J Immunol. 2014; 44:2567–2570. [PubMed: 25154881]

32. Romero P, Valmori D, Pittet MJ, Zippelius A, Rimoldi D, Levy F, Dutoit V, Ayyoub M, Rubio-Godoy V, Michielin O, Guillaume P, Batard P, Luescher IF, Lejeune F, Lienard D, Rufer N, Dietrich PY, Speiser DE, Cerottini JC. Antigenicity and immunogenicity of Melan-A/MART-1 derived peptides as targets for tumor reactive CTL in human melanoma. Immunol Rev. 2002; 188:81–96. [PubMed: 12445283]

33. Joffre OP, Segura E, Savina A, Amigorena S. Cross-presentation by dendritic cells. Nat Rev Immunol. 2012; 12:557–569. [PubMed: 22790179]

34. Chauvin JM, Larrieu P, Sarrabayrouse G, Prevost-Blondel A, Lengagne R, Desfrancois J, Labarriere N, Jotereau F. HLA anchor optimization of the melan-A-HLA-A2 epitope within a long

peptide is required for efficient cross-priming of human tumor-reactive T cells. J Immunol. 2012; 188:2102–2110. [PubMed: 22291187]

35. Rosalia RA, Quakkelaar ED, Redeker A, Khan S, Camps M, Drijfhout JW, Silva AL, Jiskoot W, van Hall T, van Veelen PA, Janssen G, Franken K, Cruz LJ, Tromp A, Oostendorp J, van der Burg SH, Ossendorp F, Melief CJ. Dendritic cells process synthetic long peptides better than whole protein, improving antigen presentation and T-cell activation. Eur J Immunol. 2013; 43:2554–2565. [PubMed: 23836147]
36. Iglesias MC, Almeida JR, Fastenackels S, van Bockel DJ, Hashimoto M, Venturi V, Gostick E, Urrutia A, Wooldridge L, Clement M, Gras S, Wilmann PG, Autran B, Moris A, Rossjohn J, Davenport MP, Takiguchi M, Brander C, Douek DC, Kelleher AD, Price DA, Appay V. Escape from highly effective public CD8+ T-cell clonotypes by HIV. Blood. 2011; 118:2138–2149. [PubMed: 21734237]
37. Glimcher LH, Townsend MJ, Sullivan BM, Lord GM. Recent developments in the transcriptional regulation of cytolytic effector cells. Nat Rev Immunol. 2004; 4:900–911. [PubMed: 15516969]
38. Takemoto N, Intlekofer AM, Northrup JT, Wherry EJ, Reiner SL. Cutting Edge: IL-12 inversely regulates T-bet and eomesodermin expression during pathogen-induced CD8+ T cell differentiation. J Immunol. 2006; 177:7515–7519. [PubMed: 17114419]
39. Breton G, Lee J, Zhou YJ, Schreiber JJ, Keler T, Puhr S, Anandasabapathy N, Schlesinger S, Caskey M, Liu K, Nussenzweig MC. Circulating precursors of human CD1c+ and CD141+ dendritic cells. J Exp Med. 2015; 212:401–413. [PubMed: 25687281]
40. Bijker MS, van den Eeden SJ, Franken KL, Melief CJ, Offringa R, van der Burg SH. CD8+ CTL priming by exact peptide epitopes in incomplete Freund's adjuvant induces a vanishing CTL response, whereas long peptides induce sustained CTL reactivity. J Immunol. 2007; 179:5033–5040. [PubMed: 17911588]
41. Melief CJ, van der Burg SH. Immunotherapy of established (pre)malignant disease by synthetic long peptide vaccines. Nat Rev Cancer. 2008; 8:351–360. [PubMed: 18418403]
42. Guiducci C, Gong M, Cepika AM, Xu Z, Tripodo C, Bennett L, Crain C, Quartier P, Cush JJ, Pascual V, Coffman RL, Barrat FJ. RNA recognition by human TLR8 can lead to autoimmune inflammation. J Exp Med. 2013; 210:2903–2919. [PubMed: 24277153]
43. Liu H, Moynihan KD, Zheng Y, Szeto GL, Li AV, Huang B, Van Egeren DS, Park C, Irvine DJ. Structure-based programming of lymph-node targeting in molecular vaccines. Nature. 2014; 507:519–522. [PubMed: 24531764]
44. Jeanbart L, Ballester M, de Titta A, Corthesy P, Romero P, Hubbell JA, Swartz MA. Enhancing efficacy of anticancer vaccines by targeted delivery to tumor-draining lymph nodes. Cancer immunology research. 2014; 2:436–447. [PubMed: 24795356]

Europe PMC Funders Author Manuscripts

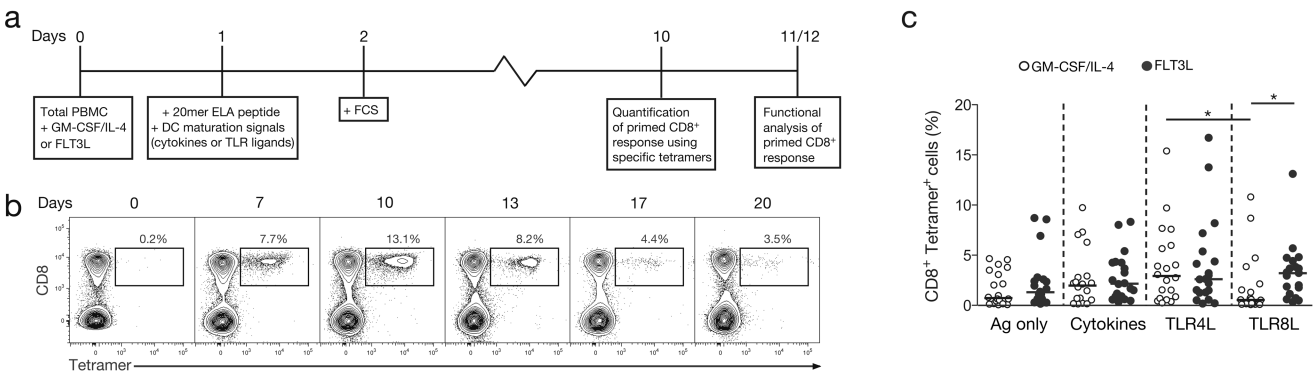

Figure 1. *In vitro* CD8$^+$ T cell priming and magnitude of TLR8L primed antigen specific cells

A. Outline of the *in vitro* CD8$^+$ T cell priming system using unfractionated PBMC samples. **B.** Representative flow cytometry data showing the kinetics of ELA-specific CD8$^+$ T cell priming in the presence of GM-CSF/IL-4 and a cocktail of inflammatory cytokines. Plots are gated on viable CD3$^+$ lymphocytes after aggregate exclusion. Numbers refer to percentages of ELA-HLA-A2 tetramer$^+$ cells within the total CD8$^+$ T cell population. **C.** Response magnitudes for ELA-specific CD8$^+$ T cell populations primed under different conditions from several healthy HLA-A2$^+$ donor PBMC samples. Antigen only (no maturation signal), cytokine cocktail (TNF, IL-1β, PGE2 and IL-7), TLR4L (LPS) or TLR8L (ssRNA40) were each used in combination with either GMCSF/IL-4 or FLT3L supplementation. Horizontal bars indicate median values. Statistical comparisons between groups were performed using the Wilcoxon signed rank test; *P < 0.05.

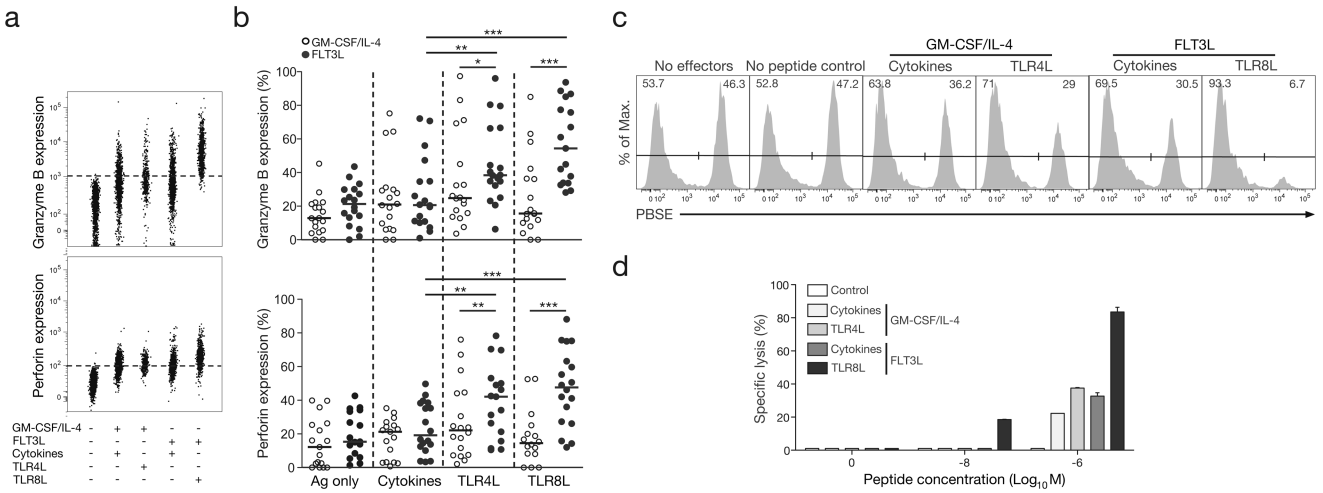

Figure 2. Greater cytotoxic potential of CD8$^+$ T cells primed *in vitro* with an FLT3L/TLR8L combination

A. Representative flow cytometry plots showing granzyme B (top panel) or perforin (bottom panel) expression by ELA-specific CD8$^+$ T cells primed under different conditions. **B.** Granzyme B (top graph) and perforin (bottom graph) expression by ELA-specific CD8$^+$ T cells primed under different conditions from several healthy HLA-A2$^+$ donor PBMC samples. Horizontal bars indicate median values. Statistical comparisons between groups were performed using the Wilcoxon signed rank test; *P < 0.05, **P < 0.01, ***P < 0.001. **C.** Representative flow cytometry data from a FATAL cytotoxicity assay showing the disappearance of ELA peptide-pulsed PBSE$^+$ HLA-A2$^+$ B-LCL target cells relative to non-peptide-pulsed PBSE- HLA-A2$^+$ B LCL control cells in the presence of ELA-specific CD8$^+$ T cells primed under different conditions. Numbers indicate the percentages of control (upper left) and target (upper right) B-LCL cells. **D.** Specific lysis of HLA-A2$^+$ B-LCL target cells presenting the indicated concentrations of exogenously-loaded ELA peptide in the presence of ELA-specific CD8$^+$ T cells primed under different conditions. A non-cognate population of CD8$^+$ T cells derived from the same HLA-A2$^+$ donor and cultured under similar conditions to the ELA-specific CD8$^+$ T cell population was used as a control. Error bars represent SD from the mean of two replicates.

Europe PMC Funders Author Manuscripts

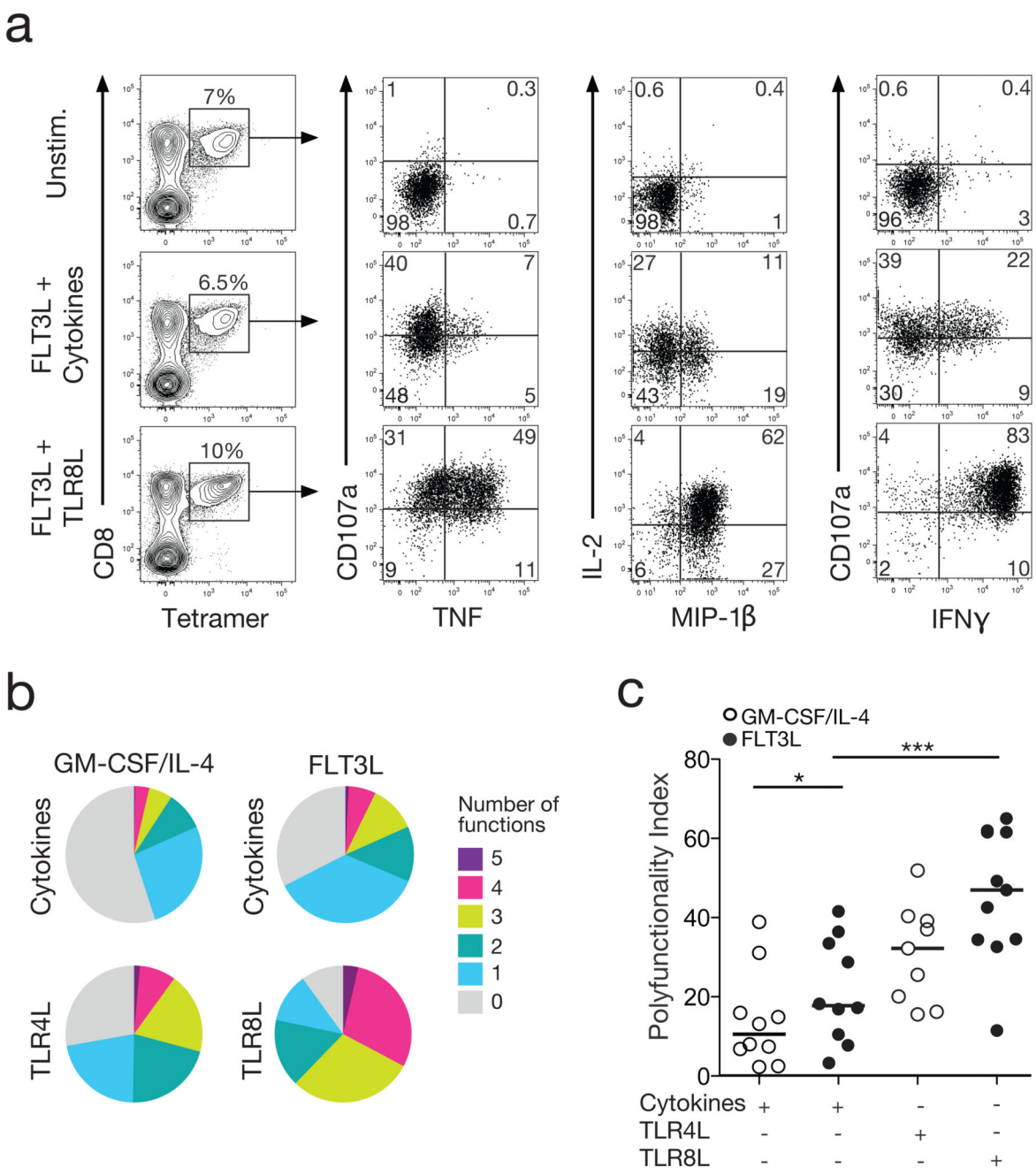

Figure 3. Polyfunctionality of FLT3L/TLR8L primed CD8$^+$ T cells

A. Representative flow cytometry plots showing cytokine production (IFNγ, MIP-1β, TNF and IL-2) and degranulation (CD107a) in response to antigen stimulation. ELA-specific CD8$^+$ T cells primed under the indicated conditions were incubated with media alone (top row) or ELA peptide-pulsed HLA-A2$^+$ B-LCL target cells (middle and bottom rows). Primed ELA-specific CD8$^+$ T cells were quantified as tetramer$^+$ cells within the total CD8$^+$ population (left column). Function plots are gated on viable CD3$^+$ CD8$^+$ tetramer$^+$ lymphocytes (middle and right columns). Numbers in each quadrant refer to the percentages

of primed ELA-specific $CD8^+$ T cells expressing the indicated combinations of functions. **B.** Averaged pie chart representations of background-adjusted polyfunctional profiles for ELA-specific $CD8^+$ T cells primed under different conditions from 10 healthy donors. Pie segments and colours correspond to the proportions of ELA-specific $CD8^+$ T cells expressing the indicated number of functions, respectively. **C.** Polyfunctionality indices for ELA-specific $CD8^+$ T cell populations, calculated from the data depicted in (B). Horizontal bars indicate median values. Statistical comparisons between groups were performed using the Wilcoxon signed rank test; *$P < 0.05$, ***$P < 0.001$.

Europe PMC Funders Author Manuscripts

Europe PMC Funders Author Manuscripts

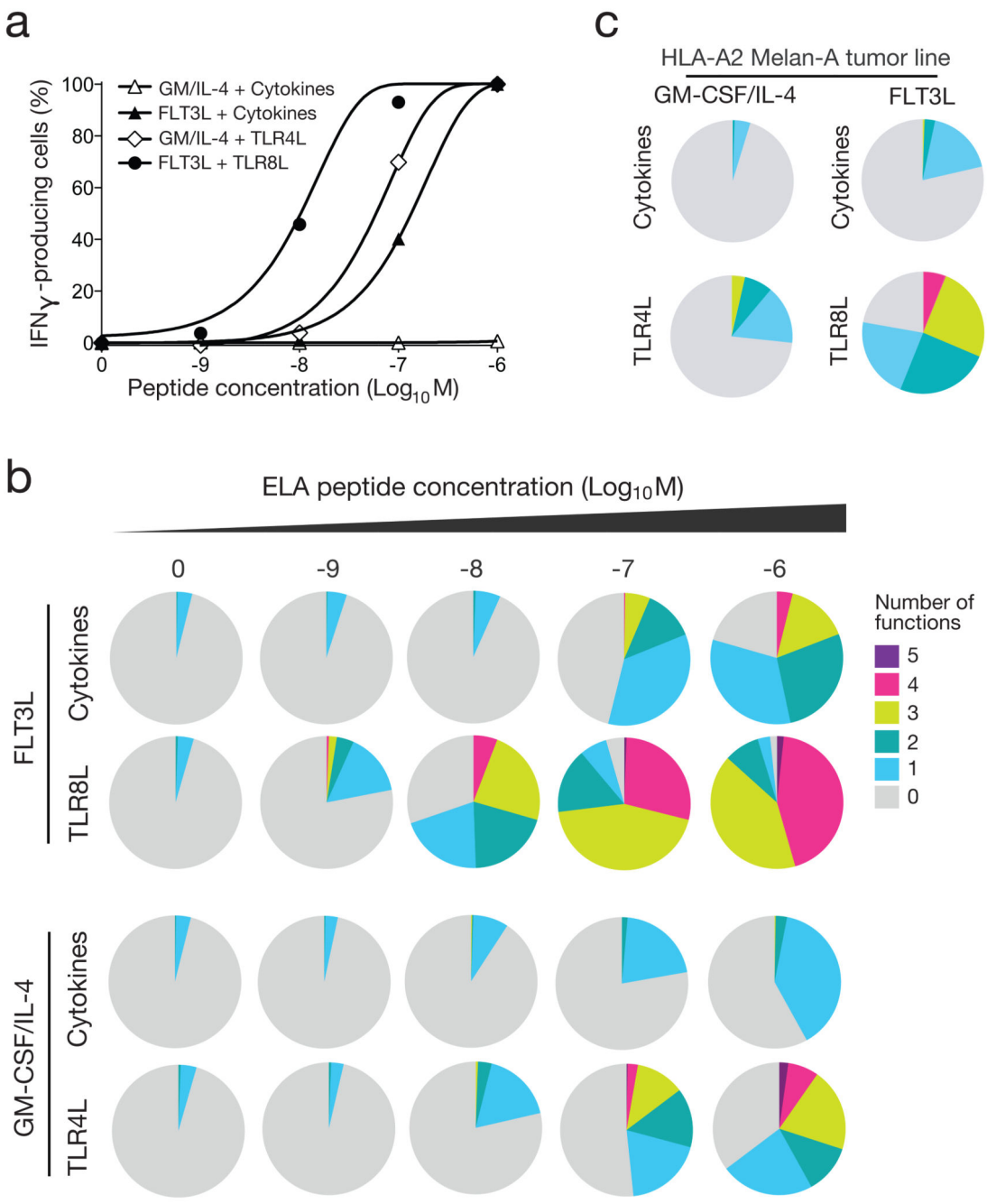

Figure 4. High antigen sensitivity of FLT3L/TLR8L primed CD8$^+$ T cells

A. Normalized IFNγ production curves for ELA-specific CD8$^+$ T cells primed under different conditions. HLA-A2$^+$ B-LCL target cells were pulsed with ELA peptide across a range of concentrations and used to stimulate ELA-specific CD8$^+$ T cells in standard intracellular cytokine staining assays. Data are representative of two independent experiments **B.** Polyfunctional profiles of ELA-specific CD8$^+$ T cells primed under the indicated conditions. HLA-A2$^+$ B-LCL target cells were pulsed with ELA peptide across a range of concentrations and used to stimulate ELA-specific CD8$^+$ T cells prior to flow

cytometric analysis. **C.** Polyfunctional profiles of ELA-specific $CD8^+$ T cells responding to natural levels of the Melan-A/MART-1 antigen presented by an $HLAA2^+$ melanoma cell line. An HLA-$A2^+$ Melan-A/MART-1^- tumor cell line was used as a negative control (data not shown). Data in (B) and (C) are depicted in pie chart representations averaged from two independent experiments conducted with HLA-$A2^+$ PBMCs from two different donors with frequencies of expanded cells equivalent in the different conditions tested.

Europe PMC Funders Author Manuscripts

Europe PMC Funders Author Manuscripts

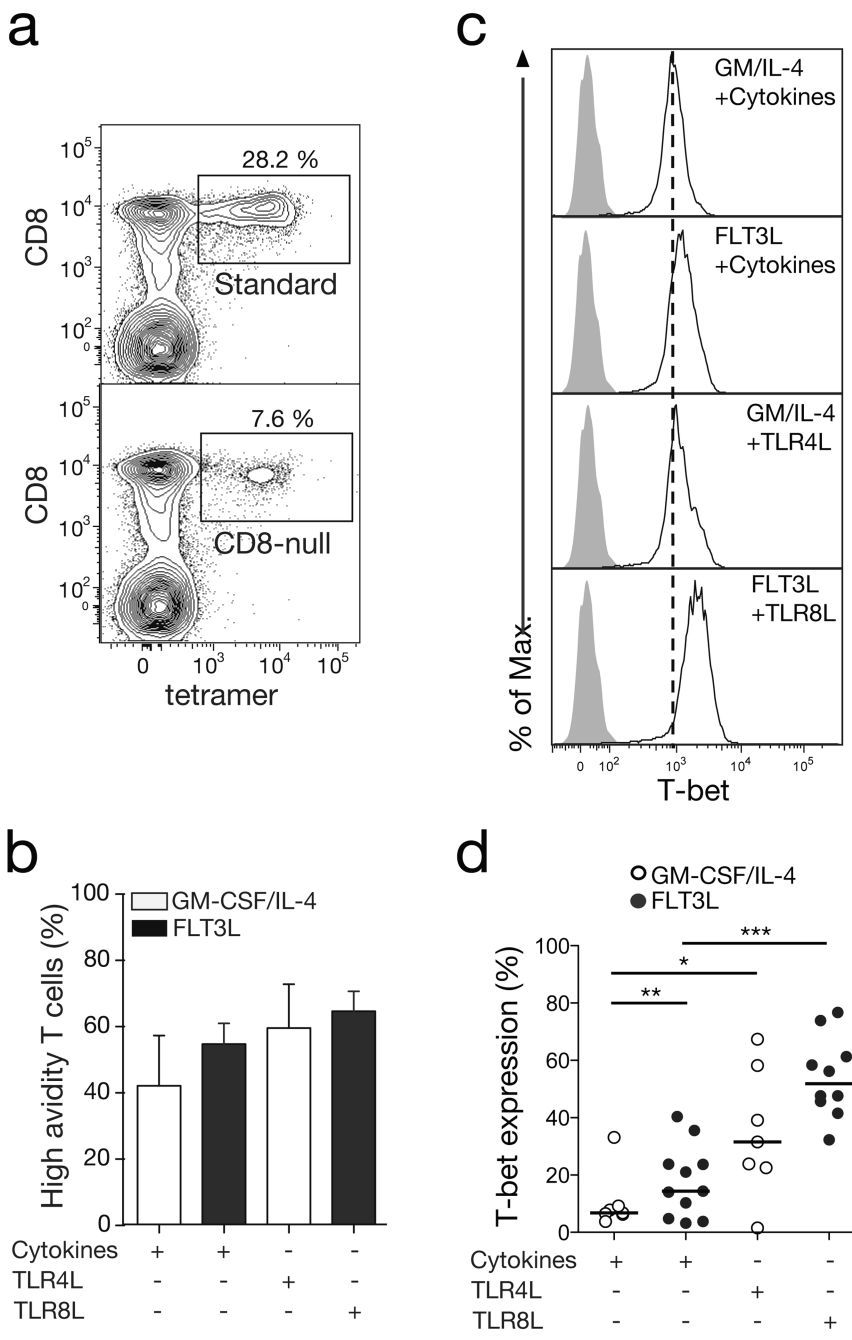

Figure 5. TCR avidity and T-bet expression in *in vitro* primed CD8$^+$ T cells

A. Representative flow cytometry plots showing standard or CD8-null ELA/HLA-A2 tetramer staining of primed ELA-specific CD8$^+$ T cells. Plots are gated on viable CD3$^+$ lymphocytes after aggregate exclusion. Numbers refer to percentages of tetramer$^+$ cells within the total CD8$^+$ population. **B.** Percentages of high avidity ELA-specific CD8$^+$ T cells primed using either GMCSF/IL-4 or FLT3L in combination with a cocktail of inflammatory cytokines (TNF, IL-1β, PGE2 and IL-7) or TLR ligands. These percentages were calculated from the corresponding CD8-null/standard ELA/HLA-A2 tetramer$^+$ cell ratios. Data are

averaged over four independent experiments. Error bars represent SD from the mean. **C.** Representative flow cytometry plots showing intracellular T-bet expression (white histograms) by ELA-specific $CD8^+$ T cells primed under different conditions. Grey histograms depict isotype control staining and vertical dotted lines indicate the mean fluorescence intensity (MFI) of T-bet staining for the weakest priming condition. **D.** Intracellular T-bet expression by ELA-specific $CD8^+$ T cells primed under different conditions. Horizontal bars indicate median values. Statistical comparisons between groups were performed using the Wilcoxon signed rank test; *P < 0.05, **P < 0.01, ***P < 0.001.

Europe PMC Funders Author Manuscripts

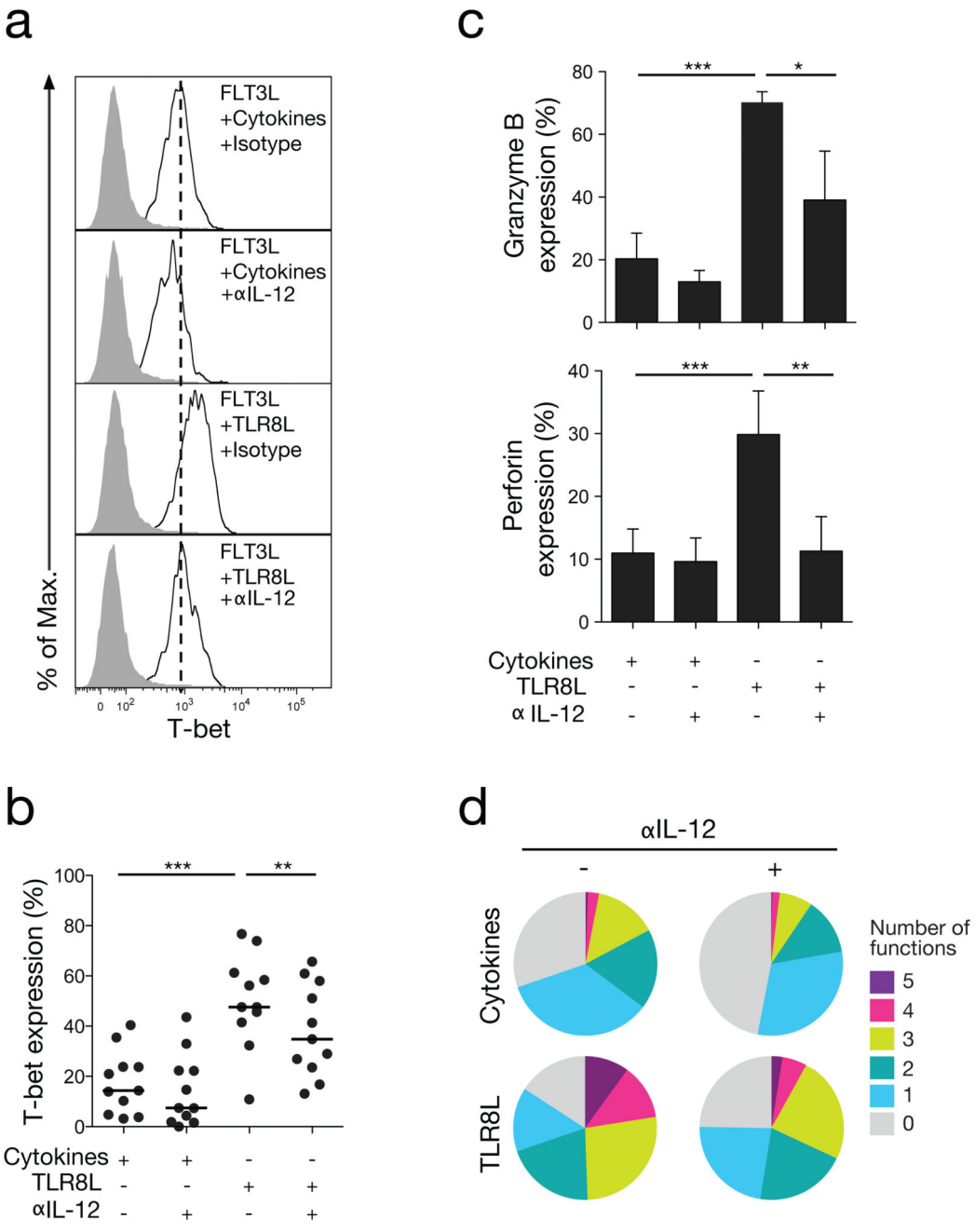

Figure 6. IL-12 dependent functional quality of FLT3L/TLR8L-primed CD8$^+$ T cells

A. Representative flow cytometry plots showing intracellular T-bet expression (white histograms) by ELA-specific CD8$^+$ T cells primed with FLT3L plus the indicated maturation signals in the presence of an α-IL-12p70 blocking antibody or a mouse IgG1 isotype control antibody. Grey histograms depict isotype control staining and vertical dotted lines indicate the mean fluorescence intensity (MFI) of T-bet staining for the weakest priming condition. **B.** Intracellular T-bet expression by ELA-specific CD8$^+$ T cells primed under different conditions. Horizontal bars indicate median values. **C.** Granzyme B (top graph) and perforin

(bottom graph) expression by ELA-specific $CD8^+$ T cells primed as in (B). Data are averaged over eight independent experiments. Error bars indicate SD from the mean. Statistical comparisons between groups were performed using the Wilcoxon signed rank test; *P < 0.05, **P < 0.01, ***P < 0.001. **D.** Polyfunctional profiles of ELA-specific $CD8^+$ T cells primed as in (B). Data are averaged over two independent experiments with ELA peptide-pulsed $HLA\text{-}A2^+$ B-LCL target cells.

Europe PMC Funders Author Manuscripts